

Supporting Information for

ORIGINAL ARTICLE

Nanoplateletsomes restrain metastatic tumor formation through decoy and active targeting in a preclinical mouse model

Longlong Zhang^{a,b,†}, Yuefei Zhu^{a,†}, Xunbin Wei^c, Xing Chen^{a,b}, Yang Li^{a,b}, Ying Zhu^a, Jiaxuan Xia^a, Yiheng Huang^a, Yongzhuo Huang^d, Jianxin Wang^{a,b,e,*}, Zhiqing Pang^{a,b,*}

^a*Department of Pharmaceutics, School of Pharmacy, Fudan University, Shanghai 201203, China*

^b*Key Laboratory of Smart Drug Delivery, Ministry of Education, Shanghai 201203, China*

^c*State Key Laboratory of Oncogenes and Related Genes, Shanghai Cancer Institute, Med-X Research Institute and School of Biomedical Engineering, Shanghai Jiao Tong University, Shanghai 200030, China*

^d*State Key Laboratory of Drug Research, Shanghai Institute of Materia Medica, Chinese Academy of Sciences Shanghai 201203, China*

^e*Institute of Materia Medica, Academy of Chinese and Western Integrative Medicine, Fudan University, Shanghai 201203, China*

Received 19 October 2021; received in revised form 16 December 2021; accepted 30 December 2021

* Corresponding authors.

E-mail addresses: zqpang@fudan.edu.cn (Zhiqing Pang), jxwang@fudan.edu.cn (Jianxin Wang).

[†]These authors made equal contributions to this work.

Running title: Nanoplateletsomes restrain metastatic tumor formation in a preclinical mouse model

1. Method

1.1. Binding of P-Lipo with tumor cells

To further ascertain the colocalization of platelet membranes and lipid membranes in the nanoplateletsome, the double-stained P-Lipo were co-cultured with 4T1 cells for 1 h in an ice bath, washed with PBS, stained with DAPI, and then imaged under the confocal laser scanning microscope with 63 × oil objective (CLSM, Zeiss LSM 710, Germany). The fluorescence intensity and colocalization coefficient were measured and analyzed by the Image J software.

1.2. Binding of P-Lipo with cells in a co-culture cell model

An HUVEC and 4T1-GFP tumor cell co-culture model was established to evaluate P-Lipo binding ability with CTCs and vessel endothelial cells in the pre-metastasis environment¹. Briefly, equal numbers of HUVECs and 4T1-GFP (2.5×10^4 cells per well) were seeded in 24 well plates and cultured overnight. The cells of approximately 80% confluence were incubated with DiD-labeled P-Lipo (or Lipo) at the DiD concentration of 50 ng/mL for 2 h at 4 °C, fixed with 4% paraformaldehyde for 15 min, stained with 5 µg/mL of Hoechst for 10 min, and then observed through an inverted microscope system (Eclipse Ti2, Nikon, Japan).

1.3. Quantitative proteomics of P-Lipo

P-Lipo or platelet membranes were resuspended 50 mmol/L ammonium bicarbonate buffer (ABC) (pH 8) in a low binding Eppendorf tube and then incubated with 5 mmol/L dithiothreitol (DTT) at 60 °C for 1 h. Afterward, 15 mmol/L iodoacetamide (IAA) was added and incubated at 20 °C in the dark for 1 hour. Then, 15 µL of 125 mmol/L cysteine was added to remove the excess IAA. Proteins were precipitated with the mixture of methanol and 50 mmol/L ABC (60:40 v/v) by ultrasonication for 5 min. Then proteins were added with 50 mmol/L ABC to decrease the methanol

concentration to 10%, followed by trypsin digestion (25 ng/ μ L) at 37 °C overnight with gently shaking. Reactions were stopped by adding 0.5% trifluoroacetic acid (TFA) to decrease the pH to 2.

Mass spectrometry data was acquired by Thermo Scientific Orbitrap Fusion Lumos (Thermo Scientific, Germany) Tribrid with NanoAcquity UPLC system (Waters, USA) equipped with a nano-electrospray ion source. The UPLC system was equipped with a 100 μ m \times 2 cm Acclaim PepMap RSLC C18 trapping column (Thermo Scientific) and a 75 μ m \times 250mm Acclaim PepMap C18 analytical column (Thermo Scientific). Loading solvent was 0.1% Formic Acid (FA) and analytical solvent was the mixture of solvent A (0.1% FA) and solvent B (99.9% acetonitrile + 0.1% FA), respectively. All separations were carried out at 45 °C. Samples were loaded at 10 μ L/min for 3 min in the loading solvent before beginning the analytical gradient. The sample was analyzed on the following linear-gradient, 5%–30% solvent B over 110 min, followed by a 4 min wash at 95% solvent B and equilibration at initial conditions for 15 min. The flow rate was maintained at 300 nL/min. Capillary voltage for ionization was set at 2 kV, and the inlet capillary temperature was maintained at 300 °C. For Orbitrap Lumos MS experiments: Precursor mass spectra were recorded in a 350 to 1550 m/z (mass/charge ratio) mass range at 120,000 resolution (at m/z 200) and 17,500 resolution for fragment ions, normalized collision energy (NCE) 35) with a top-speed approach, 1×10^6 AGC target, 120 ms maximum injection time. Typical MS setting: 2×10^5 AGC target, 100 ms maximum injection, 50,000 intensity threshold for the fragmentation. Dynamic exclusion was set to ± 10 ppm for 24 s. MS/MS fixed first mass was set at 110.

Proteomics Analysis protocols employed were similar to previous studies² with slight modifications. ProteinLynx Global Server (PLGS v2.4; Waters Corp) software was used to analyze the data collected by MS. The database used in MaxQuant (version 1.6.1.0) searches from UniProt/GO (<http://www.uniprot.org/>; <http://www.geneontology.org/>) information and manually searching in literature.

Proteins were grouped to satisfy the parsimony principle. The proteins were clustered based on biological process, and heat maps representing differentially regulated proteins by GELNs were generated using the Origin software (normalized to array reference).

1.4. Scanning electron microscope imaging of tumor cells binding with P-Lipo

Briefly, 2×10^5 4T1 cells were seeded in 24-well plates containing glass slides and cultured overnight. Afterward, 100 μg of DiD-labeled P-Lipo (or Lipo) was added, and cells were incubated for 2 h. The cell-containing glass slides were pre-fixed with 2.5% glutaraldehyde (GA) for 60 min at room temperature, washed three times with PBS, fixed with 1% osmium tetroxide (OsO_4) for 60 min, washed with PBS and deionized water twice in sequence. Then, cell samples were dehydrated with various concentrations of ethanol solutions (25%, 50%, 75%, 95% ETOH, 1×5 min, and 100% ETOH, 3×10 min) in sequence, and freeze-dried. Afterward, cells on glass slips were treated with gold spray, and observed with a scanning electron microscope imaging (SEM, FEI XL30, USA) at an operating voltage of 3 kV.

1.5. Cell apoptosis assay

The cell apoptosis of CTCs after incubation with P-Lipo was performed by flow cytometry. To obtain an artificial CTC-containing blood sample, approximately 1×10^6 4T1 cells were suspended in the whole blood diluent. Afterward, 100 μL of P-Lipo or Lipo was added into the cell suspension and incubated for 2 h under 100 rpm. Then, the cells were washed twice with PBS and stained with Annexin V-FITC and propidium iodide (PI) for 15 min. Finally, the stained 4T1 cells were analyzed through a flow cytometer (CytoFlex S, Beckman Coulter).

1.6. Pharmacokinetic study of P-Lipo

For pharmacokinetic study, BALB/c mice were intravenously injected with 100 μ L of DiD-labeled Lipo, P^L-Lipo, P^H-Lipo (2 mg/mL of lipids), respectively ($n = 4$). The blood samples were collected at preset time points (1, 5, 15 and 30 min, 1, 3, 6, 18 and 24 h) *via* a cheek pouch puncture method. The concentration of different nanovesicles in the blood was measured a Tecan Infinite M200 Pro Multiplate Reader (Switzerland, $E_x/E_m = 640/670$ nm). Statistical moment theory was used to calculate the pharmacokinetic parameters of mean residence time (*MRT*), area under the concentration-time curve (*AUC*), half-life ($t_{1/2}$), and clearance (*CL*).

2. Results and Discussion

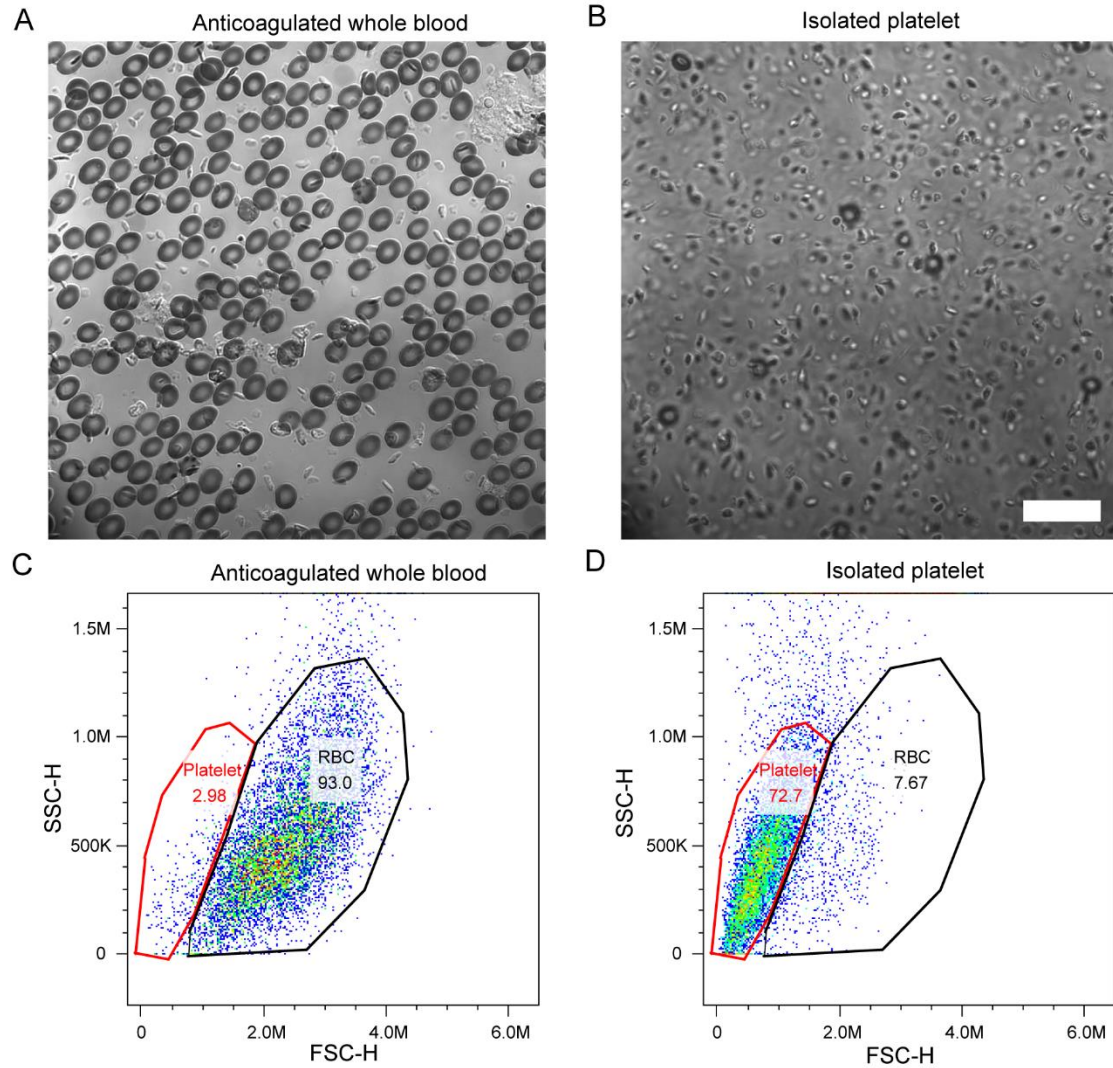


Figure S1 The identification of isolated platelets using light microscopy and flow cytometry. Light microscopy images of (A) the anti-coagulated whole blood and (B) isolated platelets at 63 × magnification. Scale bar = 20 μm. Flow cytometric analyse of (C) the anticoagulated whole blood and (D) isolated platelets.

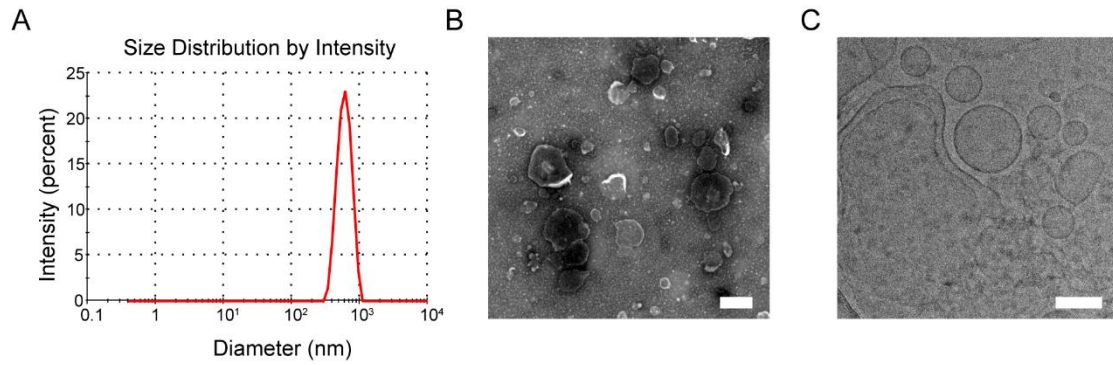


Figure S2 Characterization of platelet membranes. (A) The intensity-based particle size, (B) transmission electron microscopy images after staining with 2% uranyl, Scale bar = 0.5 μm and (C) cryogenic transmission electron microscopy images of platelet membranes, Scale bar = 0.1 μm .

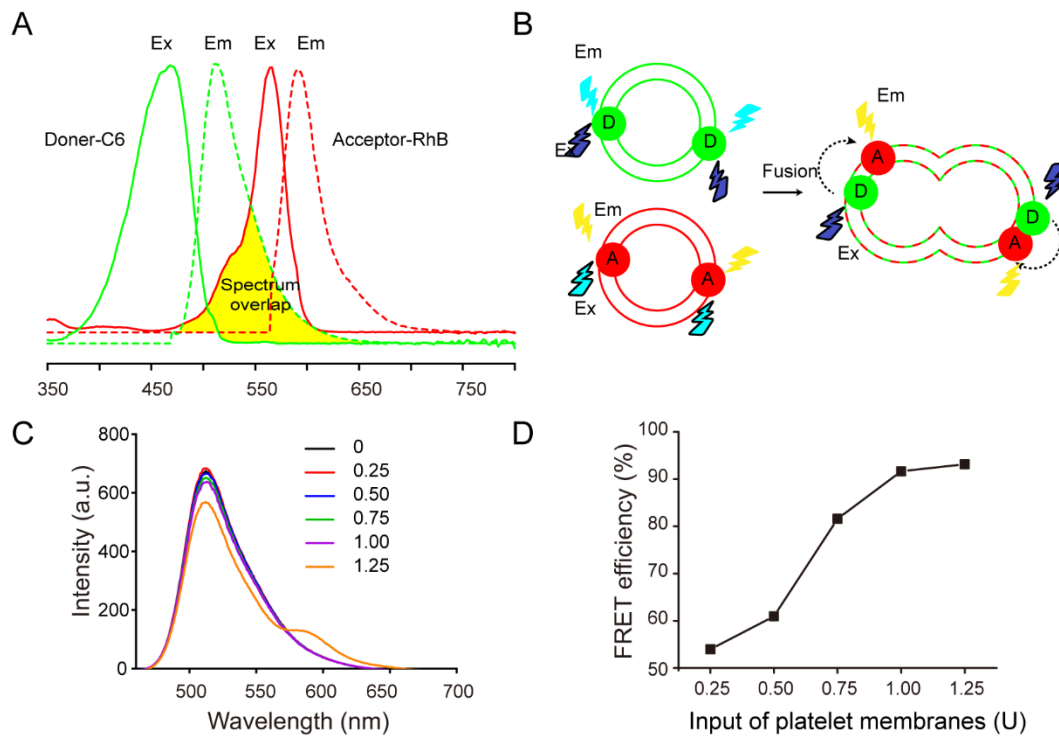


Figure S3 (A) Excitation and emission spectra of a fluorescence resonance energy transfer (FRET) donor-acceptor pair (C6-RhB). The yellow-colored region is the spectral overlap between the emission spectrum of the donor (the light green line) and the excitation spectrum of the acceptor (the solid red line). (B) Schematic illustration of FRET when the spatial distance of the donor and the acceptor was close enough,

usually < 10 nm. FRET efficiency is registered by decreased donor fluorescence intensity and increased acceptor fluorescence intensity. (C) Spectra of P-Lipo made of C6-stained lipid membranes and different amounts of RhB-labeled platelet membranes when dissolved in DMSO. (D) Calculated FRET efficiency in P-Lipo with the increasing input of platelet membranes.

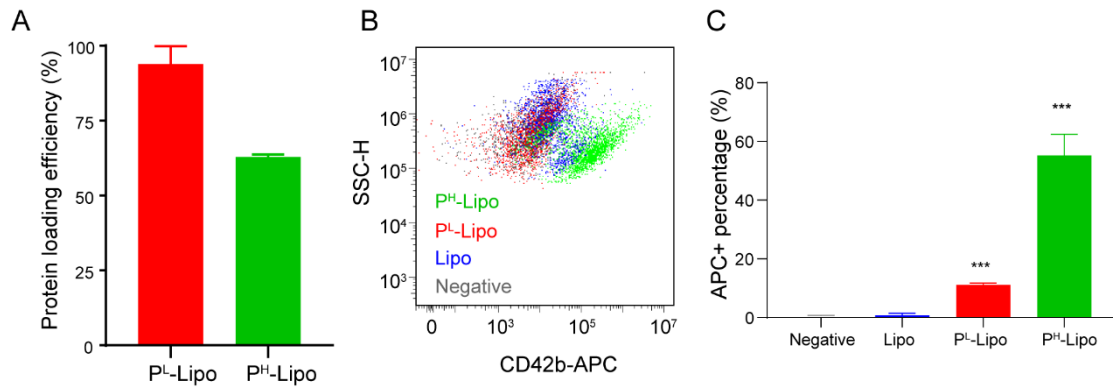


Figure S4 (A) Protein loading efficiency in P-Lipo. (B) Scatter plot of flow cytometry analysis of P-Lipo stained with anti-CD42b-APC antibody (gray dots: Control; red dots: Lipo; Blue dots: P^L-Lipo; green dots: P^H-Lipo). (C) The percentage of APC+ nanovesicles ($n = 3$). *** $P < 0.001$ compared with Lipo.

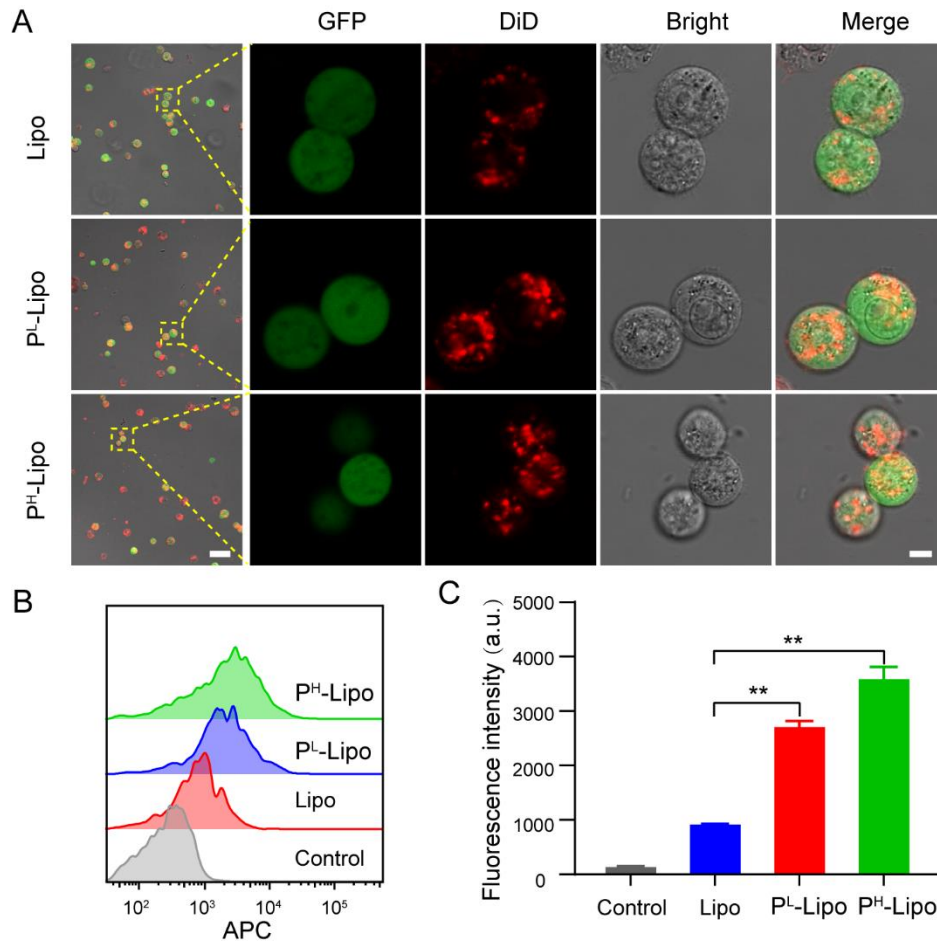


Figure S5 P-Lipo binding with CTCs in PBS. (A) Confocal laser microscopy images of tumor cells bound with P-Lipo in PBS (GFP: 4T1-GFP; DiD: DiD-labeled nanovesicles), Scale bar=50 μ m (left) and Scasle bar = 5 μ m (right). (B) The flow cytometry histogram of 4T1-GFP cells bound with DiD-labeled nanovesicles. (C) The corresponding mean fluorescence intensity of 4T1-GFP bound with DiD-labeled nanovesicles determined by flow cytometry ($n=3$). ** $P < 0.01$ compared with Lipo.

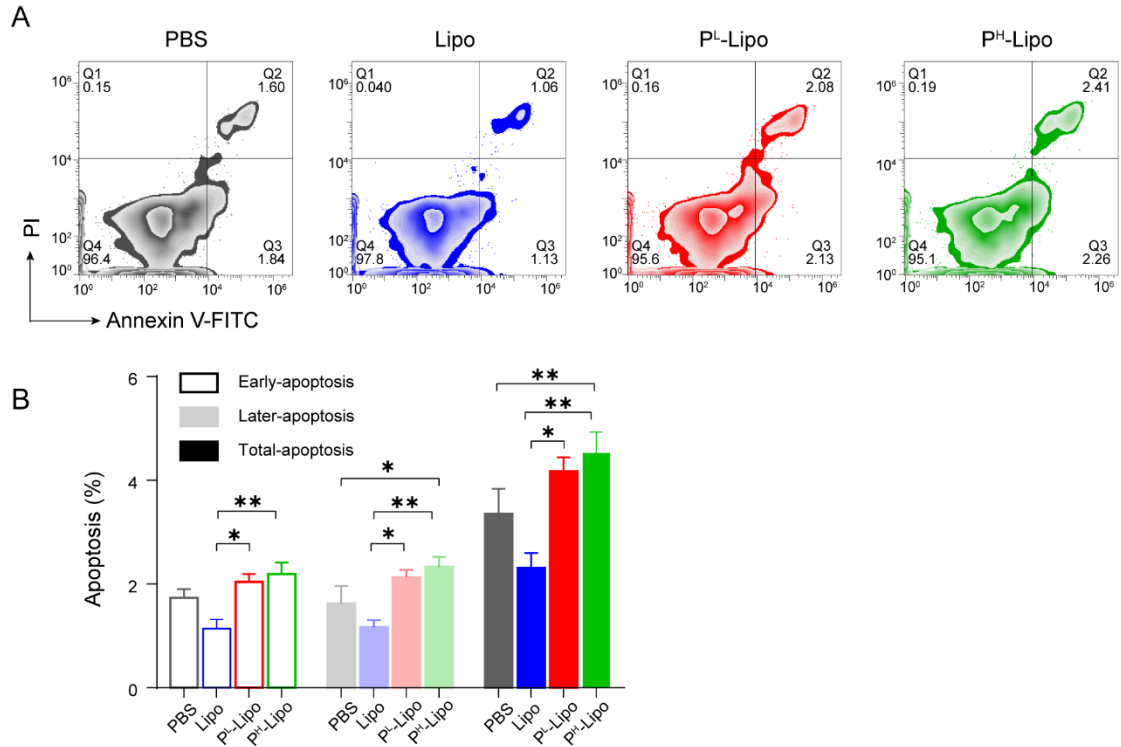


Figure S6. Flow cytometry analysis of cell apoptosis of 4T1 cells after incubation with P-Lipo in the whole blood diluent. (A) Representative flow cytometry contour plots of 4T1 cells after different treatments. Q1 represented dead cells (FITC⁻/PI⁺), Q2 represented late apoptotic cells (FITC⁺/PI⁺), Q3 represented early apoptotic cells (FITC⁺/PI⁻), Q4 represented intact cells (FITC⁻/PI⁻). (B) The cell percentages of early apoptosis, late apoptosis, and total apoptosis after different treatments ($n = 3$). * $P < 0.05$ and ** $P < 0.01$.

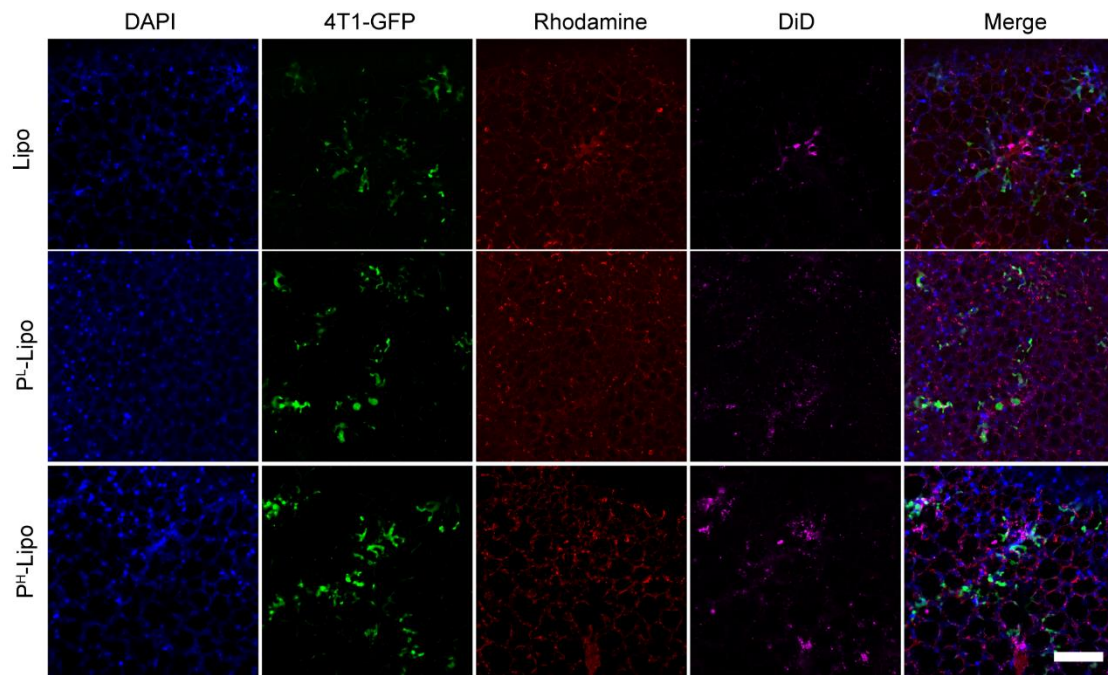


Figure S7 Fluorescence images of 4T1-GFP cells colocalized with DiD-labeled P-Lipo (or Lipo) in *ex vivo* lungs at 20 min after injection. Blue, green, red, and pinkish-red fluorescence indicated DAPI-labeled nuclei, 4T1-GFP cells, rhodamine-conjugated dextran-labeled pulmonary capillary, and DiD-labeled P-Lipo (or Lipo), respectively. Scale bar = 100 μ m.

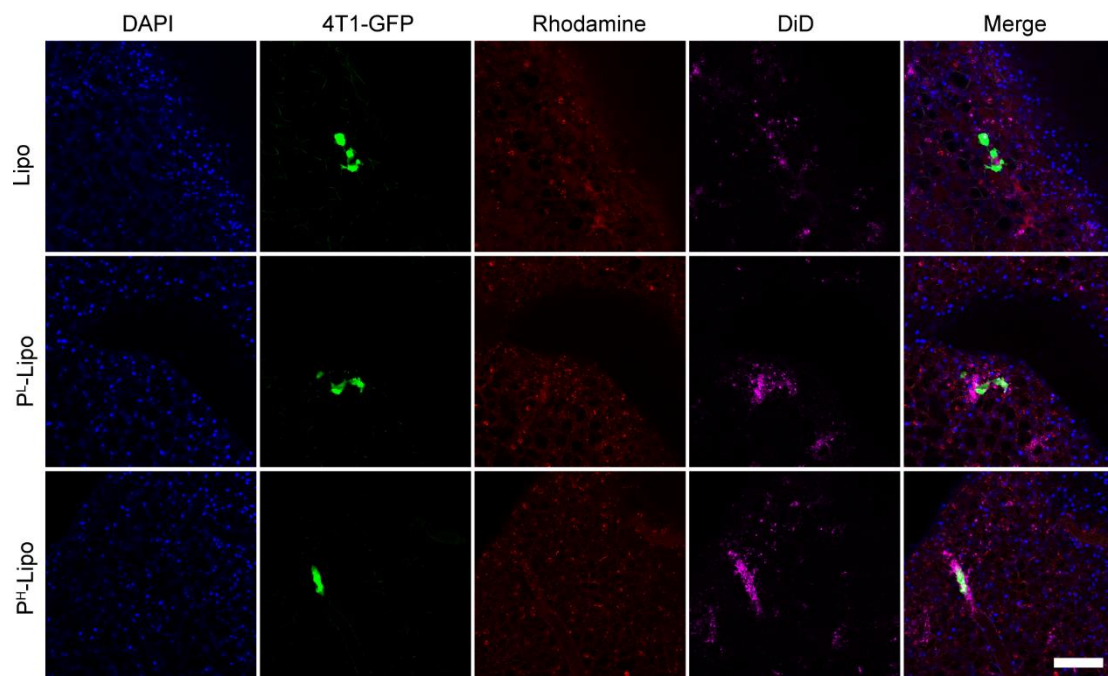


Figure S8 Fluorescence images of 4T1-GFP cells colocalized with DiD-labeled

P-Lipo (or Lipo) in *ex vivo* lungs at 24 h after injection. Blue, green, red, and pinkish-red fluorescence indicated DAPI-labeled nuclei, 4T1-GFP cells, rhodamine-conjugated dextran-labeled pulmonary capillary, and DiD-labeled P-Lipo (or Lipo), respectively. Scale bar = 100 μm .

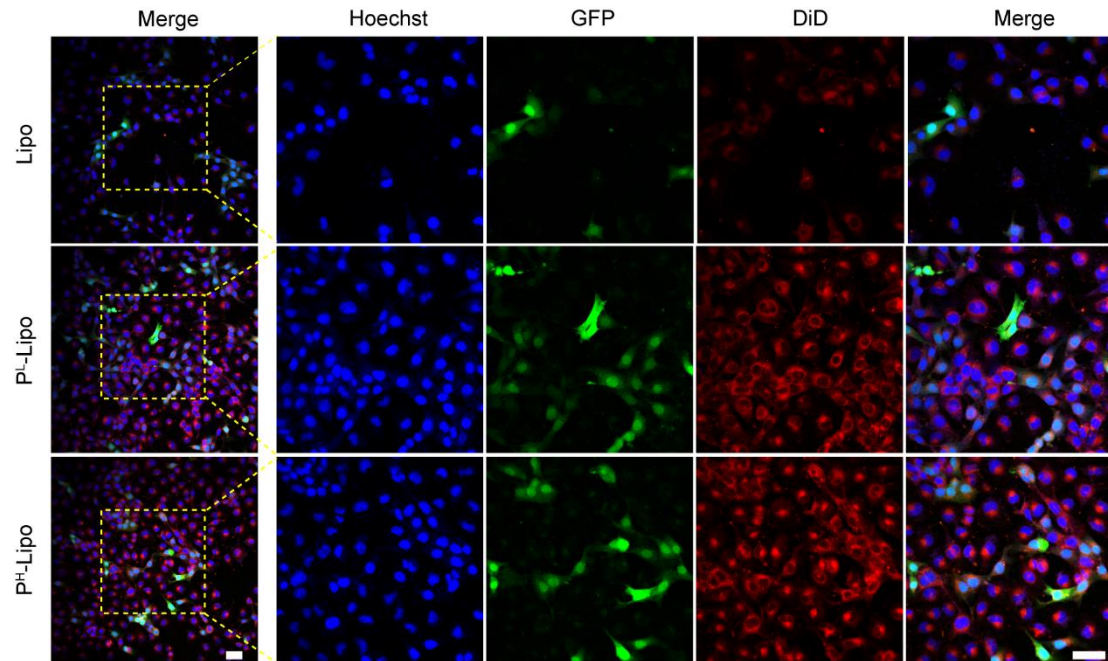


Figure S9 Cell adhesion of DiD-labeled P-Lipo (or Lipo) in the coculture model established using HUVEC and 4T1-GFP. The cells were imaged after 2 h incubation with DiD-labeled P-Lipo (or Lipo). Scale bar = 50 μm .

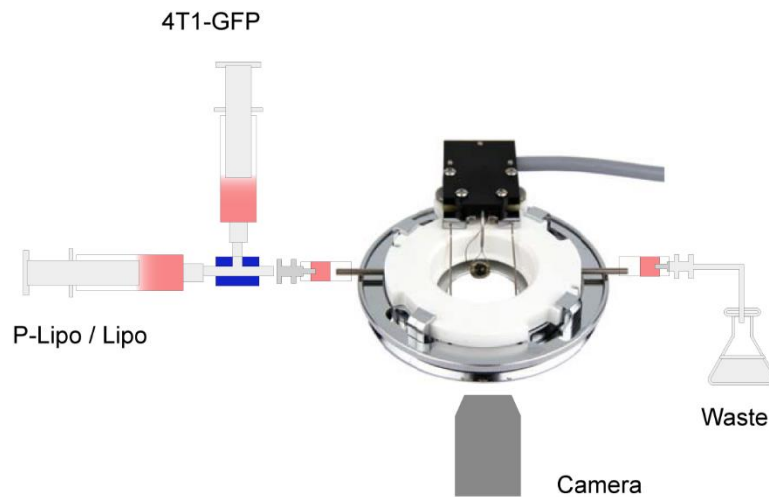


Figure S10 Focht chamber system (FCS2) configuration for *in vitro* flow-state CTC adhesion on HUVEC. Revised with permission from Biopetechs (<http://www.Biopetechs.com>)

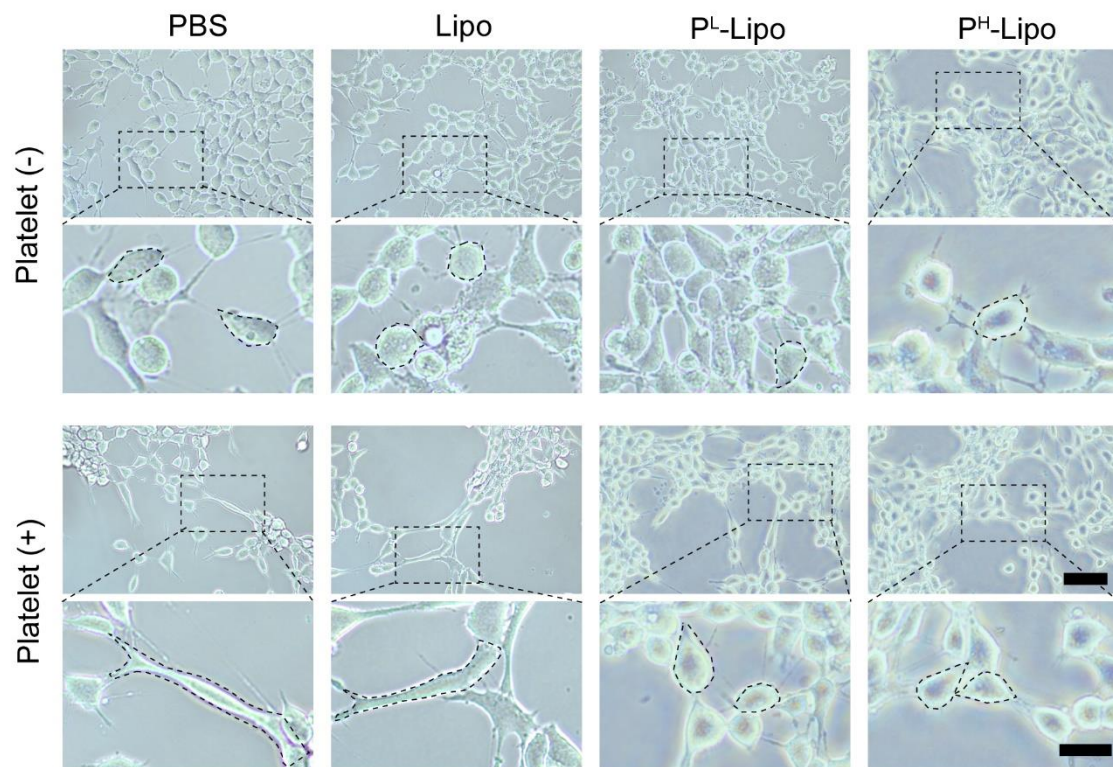


Figure S11 Morphology of 4T1 tumor cells treated with PBS, LI, P^L-Lipo, and P^H-Lipo in the presence or absence of platelets. Typical cell morphologies³ were pointed out by dotted lines. Scale bar = 50 μm (above) and Scale bar = 20 μm

(below).

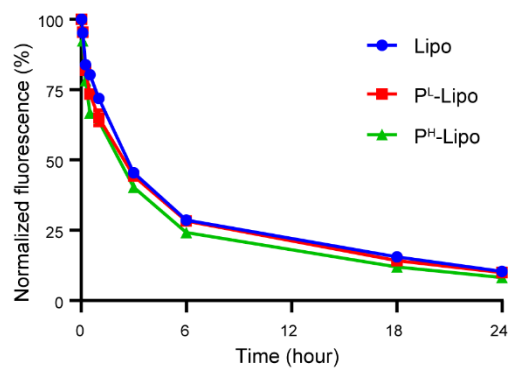


Figure S12 Pharmacokinetic curves of DiD-labeled Lipo, P^L-Lipo, P^H-Lipo after intravenous injection ($n = 5$).

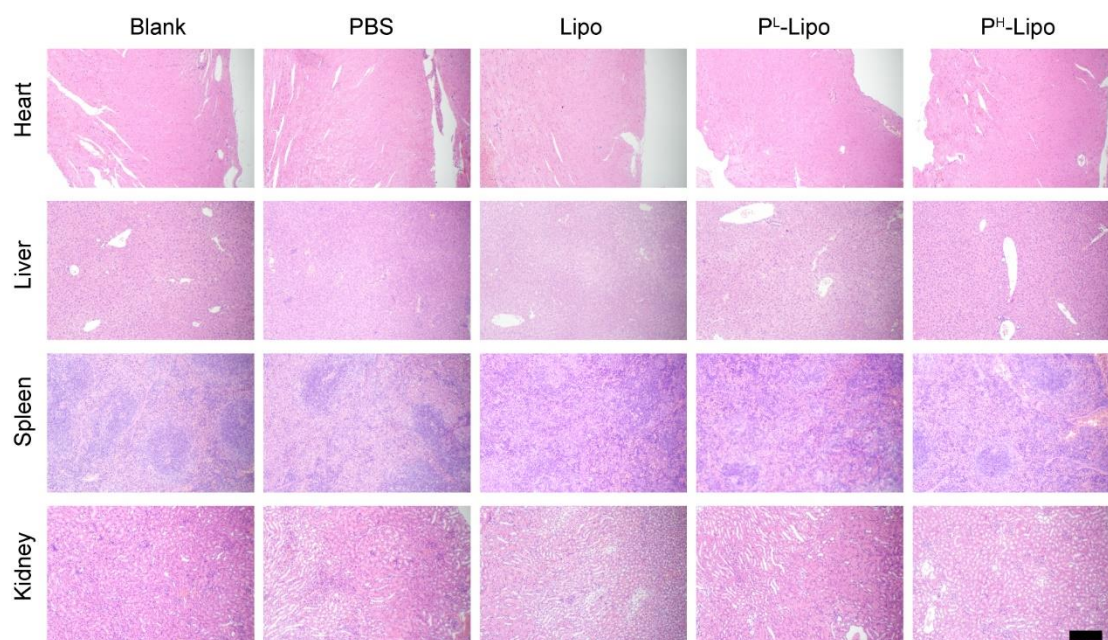


Figure S13 The hematoxylin-eosin staining images of the sections of the heart, the liver, the kidney, and the spleen from model mice on day 15 after treatment. Scale bar = 50 μm .

Table S1 Pharmacokinetic parameters of DiD-labeled Lipo, P^L-Lipo, P^H-Lipo after intravenous injection ($n = 5$).

Parameter	Lipo	P ^L -Lipo	P ^H -Lipo
$t_{1/2}$ (h)	4.68±0.20	4.67±0.38	4.33±0.57
MRT_{0-t} (h)	7.02±0.16	7.01±0.19	6.65±0.59
$MRT_{0-\infty}$ (h)	7.65±0.25	7.63±0.35	7.13±0.83
AUC_{0-t} (%ID h /mL)	643±38	609±30	546±37*
$AUC_{0-\infty}$ (%ID h /mL)	661±42	623±27	558±44*
CL (L/h/kg)	0.012±0.001	0.013±0.001	0.015±0.001*

The concentration of vesicles in the plasma was presented as %ID/mL (Percentage of injected dose per millimeter). $t_{1/2}$, half-life; MRT_{0-t} , mean residence time from time 0 to time t ; $MRT_{0-\infty}$, mean residence time from 0 h to infinity; AUC_{0-t} , area under the concentration–time curve from time 0 to time t ; $AUC_{0-\infty}$, area under the concentration–time curve from time 0 to infinity; CL , clearance. * $P < 0.05$, compared with Lipo.

Estimated surface area ratio of lipid membranes to platelet membranes

Mass of PC: $M = 758$ g per mole

Mass of cholesterol: $M = 387$ g per mole

PC molecules for 4.0 mg of PC: 3.18×10^{18}

Cholesterol molecules for 0.8 mg of cholesterol: 1.24×10^{18}

Lipid molecules for a 100-nm liposome²: $\approx 10^5$

Numbers of liposomes made of 4.0 mg of PC and 0.8 mg of cholesterol: 4.42×10^{13}

Surface area per liposome sized 100 nm: $4\pi R^2 = 3.14 \times 10^{-14} \text{ m}^2$

Total surface area of liposomes (S1): 1.39 m^2

Surface area per platelet⁴: $\approx 22.2 \text{ } \mu\text{m}^2$

Platelet count in the whole blood: $\approx 3 \times 10^8$ per mL

Total surface area of 1 mL of platelets (S₂): 0.00666 m²

Surface area ratio of lipid membranes to platelet membranes for P^L-Lipo: $S_1/(0.4 \times S_2)$
= 521

Surface area ratio of lipid membranes to platelet membranes for P^H-Lipo: $S_1/(1.6 \times S_2)$
= 130

Number ratio of P^L-Lipo or P^H-Lipo to platelets: 1.47×10^5

Estimated surface-to-volume ratio for platelets and P-Lipo

Volume per platelet⁴ : $\approx 7.1 \mu\text{m}^3$

Surface area per platelet⁴ : $\approx 22.2 \mu\text{m}^2$

Estimated surface-to-volume ratio (SVR) for platelets: 3.13

Surface area per liposome sized 100 nm: $4\pi R^2 = 3.14 \times 10^{-14} \text{m}^2$

Volume per liposome sized 100 nm: $4/3\pi R^3 = 5.23 \times 10^{-22} \text{m}^3$

Estimated surface-to-volume ratio for liposomes: 6×10^7

The SVR ratio of P-Lipo to platelets: $\approx 1.92 \times 10^7$

References

- 1 Zhang X, Wang C, Wang J, Hu Q, Langworthy B, Ye Y, et al. PD-1 blockade cellular vesicles for cancer immunotherapy. *Adv Mater* 2018;**30**:1707112–19.
- 2 He Y, Li R, Li H, Zhang S, Dai W, Wu Q, et al. Erythroliposomes: integrated hybrid nanovesicles composed of erythrocyte membranes and artificial lipid membranes for pore-forming toxin clearance. *ACS Nano* 2019;**13**:4148–59.
- 3 Xu Y, Liu J, Liu Z, Ren H, Yong J, Li W, et al. Blockade of platelets using tumor-specific NO-releasing nanoparticles prevents tumor metastasis and reverses tumor immunosuppression. *ACS Nano* 2020;**14**:9780–95.
- 4 Frojmovic MM, Panjwani R. Geometry of normal mammalian platelets by quantitative microscopic studies. *Biophys J* 1976;**16**:1071–89.